Hergert, T., Heidbach, O. (2010): Slip-rate variability and distributed deformation in the Marmara Sea fault system. - Nature Geoscience, 3, 132-135

DOI: 10.1038/ngeo739

LETTERS
PUBLISHED ONLINE: 17 JANUARY 2010 | DOI: 10.1038/NGEO739
nature geoscience

Slip-rate variability and distributed deformation in the Marmara Sea fault system

Tobias Hergert* and Oliver Heidbach*†

The slip rate along a fault controls the accumulation of strain that is eventually released during an earthquake[1]. Along a 150-km-long stretch of the North Anatolian fault near Istanbul, Turkey, strain has been building up[2] since the last large earthquake in 1766. Estimates of the geodetic slip rates along the main Marmara fault vary widely, ranging between 17 and 27.9 mm yr^{-1} (refs 2–5). This slip rate is difficult to quantify because of the lack of satellite observations offshore and the complexity of the submarine fault system that includes the main Marmara fault[2,6,7]. Here we estimate the right-lateral slip rate on the main Marmara fault using a three-dimensional geomechanical model that incorporates these structural complexities. From our simulations we infer slip rates between 12.8 and 17.8 mm yr^{-1}; our estimates are smaller and more variable than previous results, primarily because of slip partitioning and internal deformation. Our model results reconcile geodetic observations and geological fault slip rates[8–10], which had been considered conflicting previously. We suggest that the inferred variability in slip rate on the main Marmara fault favours segmented release of seismic moment during consecutive events over the failure of the whole seismic gap in one large earthquake.

The slip rate on a fault is a key parameter in estimating its seismic potential. In the absence of aseismic creep, it governs the rate of interseismic strain accumulation around a locked fault[1]. Accordingly, fault slip rates are related to recurrence rates of characteristic earthquakes that are the starting point for time-dependent seismic hazard assessment[11,12].

Along the North Anatolian fault (NAF), the Anatolian plate moves westward with respect to the Eurasian plate[13] (Fig. 1), at a rate of ~25 $mmyr^{-1}$ (ref. 5) east of the Sea of Marmara. The NAF is mainly a single vertical fault that follows the small circle of the rotation of the Anatolian plate[5]. However, the NAF splits into three main branches west of the city of Bolu, namely the main Marmara fault[2,7] (MMF) and the middle and southern branches (Fig. 1). Under the Sea of Marmara, the NAF splits further into a complex fault network with numerous fault strands of varying dip and strike[6,14]. The question arises of how relative plate motion is accommodated across the Sea of Marmara region, whether it is localized, partitioned or distributed, and in particular what the slip rate is on the MMF close to Istanbul.

To quantify the slip rate on the MMF, we set up a geomechanical model that takes into account the three-dimensional fault system as contact surfaces that allow frictional sliding according to the Coulomb criterion (see Supplementary Information). The fault geometry is derived from mapped fault traces at the sea floor[7] and seismic images of the subsurface[6,14–16] (Fig. 2a). Topography, bathymetry, basement and Moho depth are also incorporated to account for changes in elastic properties and densities (Fig. 2b,c).

Kinematic boundary conditions drive the model from its lateral boundaries so that both localized deformation on faults and distributed deformation in between faults evolve in response to these. The acting plate tectonic boundary conditions are derived from a large-scale model and are consistent with the observed velocity field of northwest Anatolia (see Supplementary Information). We applied the finite-element method using the solver Abaqus.

Our model simulates the interseismic strain accumulation observed at the global positioning system (GPS) sites by locking the faults in the seismogenic layer within the model (see Supplementary Information). This allows comparison of the modelled velocities with GPS-derived velocities. Deviations are mostly within the 95% confidence uncertainties of the observations (Fig. 3a). West-directed motion of the Anatolian plate is transferred across the locked faults to the Eurasian plate (Fig. 3a). These interseismic velocities contain the effects within a seismic cycle when faults are locked whereas fault slip rates are due to average velocities over several seismic cycles. Thus, to quantify the rate of continuous fault slip, we unlock the faults in the seismogenic layer (lowering the coefficient of friction from infinity to $\mu' = 0.05$). Except for μ', this model is identical to our previous locked-fault model; in particular, the boundary conditions are the same. This model with unlocked faults estimates that slip rates on the MMF range between 12.8 and 17.8 $mmyr^{-1}$ and are less than 4 $mmyr^{-1}$ on the other faults (Fig. 3b). The west-directed motion of the Anatolian plate is no longer transferred to the Eurasian plate in this unlocked-fault model. Analysis of the uncertainties of coefficient of friction, rock stiffness and kinematic boundary conditions shows that the MMF slip rate is at most 2 $mmyr^{-1}$ greater than the rates shown in Fig. 3b (Supplementary Fig. S4).

Geophysical Institute, Universität Karlsruhe (TH), Hertzstr. 16, 76187 Karlsruhe, Germany. † Present address: GFZ German Research Centre for Geosciences, Telegrafenberg, 14773 Potsdam, Germany. * e-mail: tobias.hergert@gpi.uni-karlsruhe.de; heidbach@gfz-potsdam.de

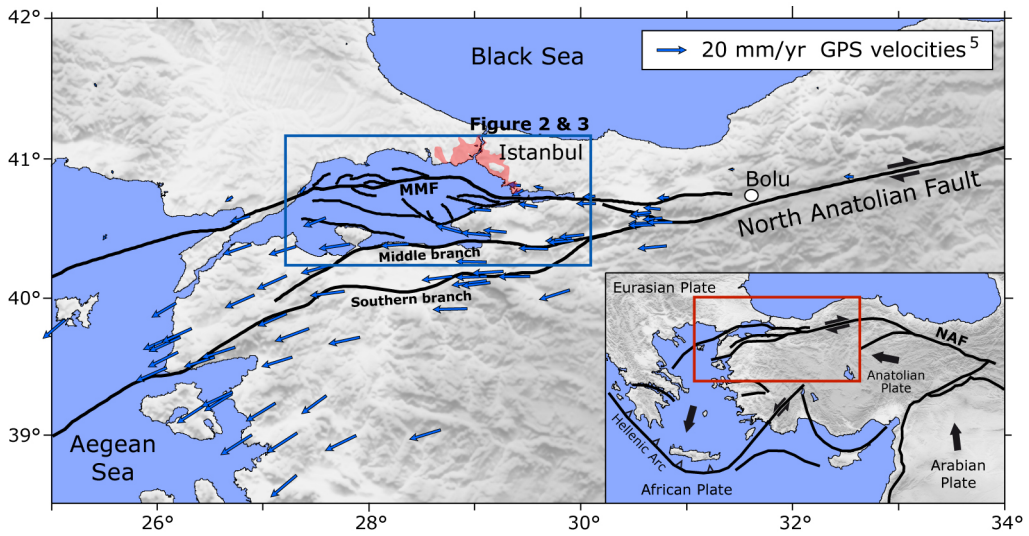

Figure 2 | Tectonic setting of Anatolia. The NAF splits several branches[7] west of the city of Bolu. The GPS-derived velocities[5] (blue arrows) relative to stable Eurasia indicate that most of the strain is accumulated below the Sea of Marmara. The blue rectangle shows the location of Figs 2 and 3. Inset: Horizontal velocities in the eastern Mediterranean are controlled by the indentation of the Arabian plate into the Eurasian plate and by the southward retreat of the Hellenic subduction zone[13]. This produces westward escape of the Anatolian plate along the NAF. The red rectangle shows the location of the main panel.

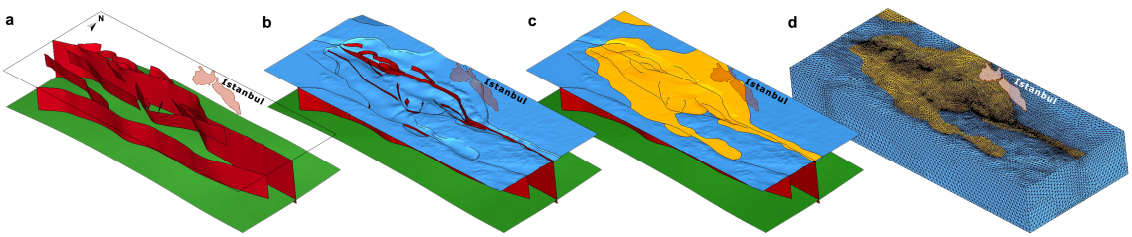

Figure 1 | Model geometry and finite-element discretization. a, The green surface shows the Moho that varies between 26 and 35km depth. The red surfaces indicate faults that dip between 70° and 90°. **b**, The blue layer is the basement topography at 0–6km depth. **c**, The yellow layer marks the Earth's surface where the basement is overlain by sediments. **d**, Volume discretization with 640,000 finite elements using HyperMesh.

The vertical velocity field predicted from the model with unlocked faults correlates well with known depocentres (particularly near the Tuzla and Ganos bends[17,18]), and with regions of uplift, such as the western shore and south of Izmit Bay[19,20] (Fig. 3c). Footwalls of main non-vertical fault segments are stable[17,18] and Marmara Island tilts towards the south[16]. This gives confidence that the implemented fault geometry is appropriate. We consider both a mechanically continuous MMF and deep-rooted second-order faults, whereas they were taken as mutually exclusive earlier[2,7].

Previous GPS-constrained models estimated right-lateral MMF slip rates of 17-20, 23, 24.4-24.8 and 24.6-27.9 mmyr^{-1} (refs 2-5). Our slip rates of 12.8-17.8 mmyr^{-1} are smaller than these by 10-45%, depending on location and study (see Supplementary Table S2). Furthermore, whereas previous estimates propose low variability[3–5] or even emphasize a constant MMF slip rate[2], our slip rate varies by 40% along strike (Fig. 3b).

The main reasons for the lower MMF slip rates predicted herein are (1) slip partitioning on second-order faults, (2) internal deformation in the rock volume between the faults and, to a lesser extent, (3) dip-slip on non-vertical fault segments that strike obliquely to plate motion (Fig. 3c). The effect of slip partitioning and internal deformation is shown in Fig. 4, where east–west velocities are presented along two north–south profiles. Whereas previous studies predicted that most fault slip occurs along the MMF, the velocity steps south of the MMF indicate that a significant amount of slip is taken up by other smaller faults (Fig. 4). Although slip rates on individual faults other than the MMF are small, their cumulative effect cannot be neglected, as they make up a substantial fraction (1−7 mm yr^{-1}) of the total relative plate motion in the Sea of Marmara area. The gradual change in east–west velocity further indicates that deformation (1−3 mmyr^{-1}) occurs between faults (Fig. 4). This internal deformation may occur through slip on smaller faults not included in the model, or rotation and permanent strain of the intrafault zone. Finally, changes in vertical velocity at the Prince's Islands segment or the western branch of the Imralı fault (Fig. 3c) indicate that a small fraction of relative plate motion is also accommodated by dip-slip on non-vertical faults.

The discrepancies among the above-mentioned studies of geodetically derived fault slip rates[2–5] including this study cannot be attributed to the GPS observations themselves because all of these studies rely on essentially the same GPS observations[5,21]. The so-called 'geodetic fault slip rate' is not an observation by itself but a derived quantity using geomechanical models. Thus, the result depends strongly on how the mechanical link between interseismic surface deformation and fault slip is established in the model. This highlights that inferring fault slip rates from geodetic observations requires adequate mechanical representation of ongoing kinematics in models, in particular detailed fault geometry.

The model results presented herein resolve the controversy surrounding the discrepancy between geologically derived slip rates of the northern branch of the

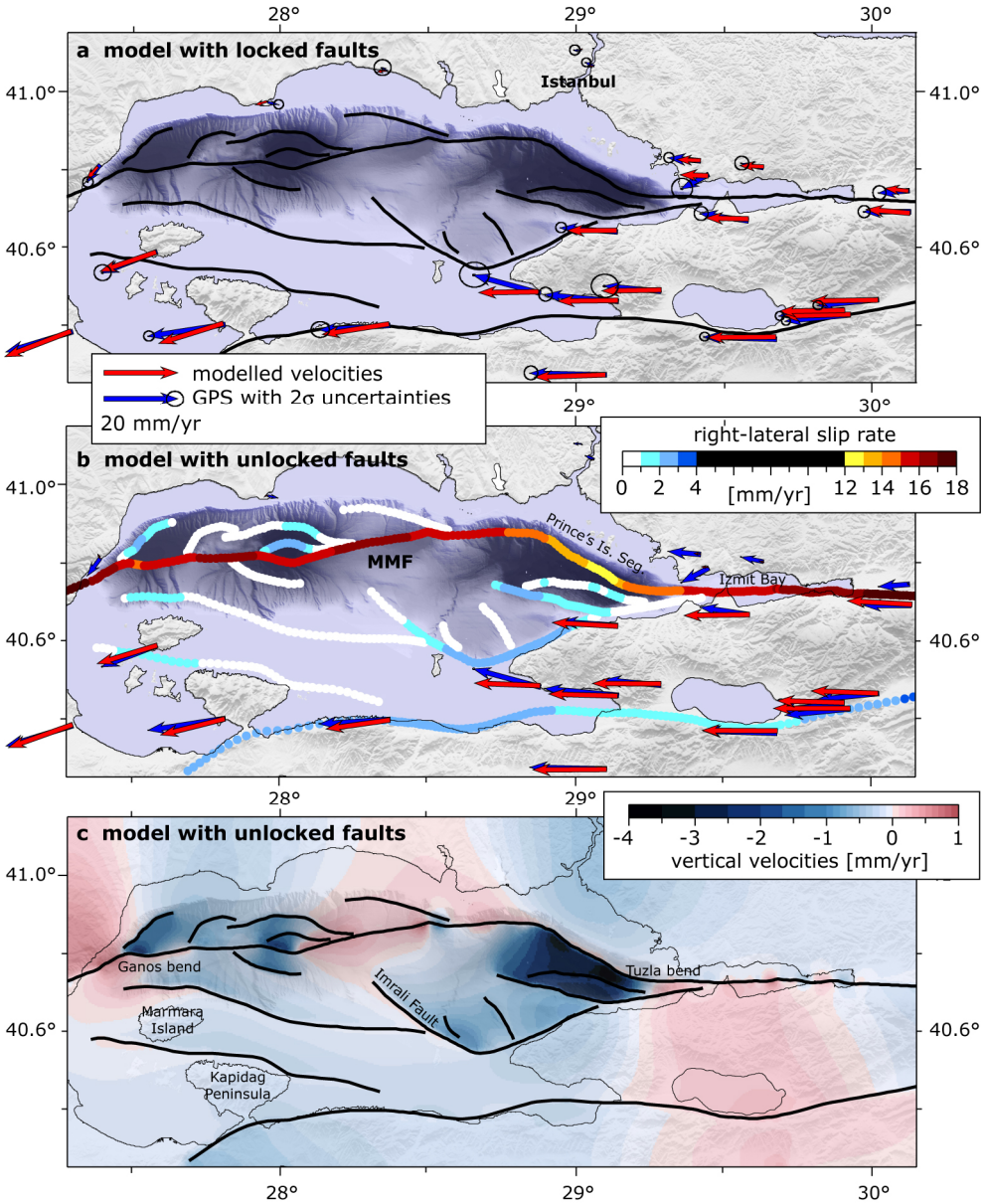

Figure 3 | Velocities and fault slip rates at the surface. a, Horizontal velocities from the model (red arrows) with faults locked in the uppermost 15 km in comparison with GPS velocities[5] (blue arrows with 2σ uncertainty ellipses[5]). **b**, Horizontal velocities from the model with unlocked faults ($\mu' = 0.05$) in comparison with GPS velocities[5]. Modelled right-lateral MMF slip rate (coloured lines) varies between 12.8 and 17.8 mmyr^{-1} at the surface and is only a little greater at depth (Supplementary Fig. S3). **c**, Vertical velocities from the model with unlocked faults.

NAF (in the range of 14−19mmyr^{-1} (refs 8–10)) and the significantly higher slip rates derived from GPS observations by means of geomechanical models (17−28 mmyr^{-1}; refs 2–5). Our modelled velocities and fault slip rates (12.8−17.8 mmyr^{-1}) agree well with the geodetic observations and with the geological fault slip rates. Neither temporal changes in fault slip rates nor erroneous geological slip rates have to be evoked to explain the apparent conflict. Both, GPS velocities and geological slip rates can be explained by incorporating the detailed three-dimensional fault geometry of the region into the model and by allowing for both localized and distributed deformation.

The lower slip rate on the MMF predicted herein suggests that the slip deficit that has accrued since the last major earthquake is smaller than previously estimated. The same applies to the recurrence rates of characteristic earthquakes if these are determined by dividing typical coseismic slip by the fault slip rate. Furthermore, the predicted changes in right-lateral slip rate along strike of the MMF implies that the rate of interseismic strain accumulation is spatially variable. Thus, critical levels of shear stress are reached at different times along the fault and failure of the whole seismic gap at once is less likely. In agreement with this, magnitudes of historical earthquakes in the Sea of Marmara were estimated to be smaller compared with where the NAF shows a simpler geometry onshore[22]. However, we must clearly point out that the seismic hazard in the Marmara Sea region is still tremendously high. The slip deficit accrued from 1766 onward on the MMF is ~4 m using our slip rate of 16 mmyr^{-1}. This is still large enough to produce $M > 7$ earthquakes depending on the length of the fault segment that will rupture, with a worst-case estimate of $M \sim 7.6$. Furthermore, dynamic stress triggering may overcome the different levels of shear stress and prolong rupture.

We conclude that total relative plate motion between the

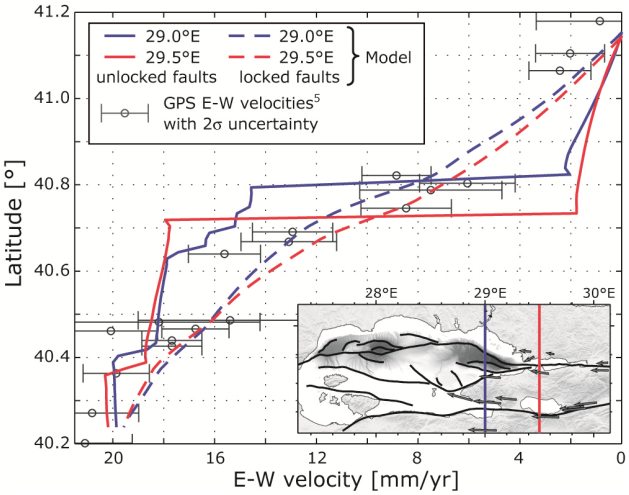

Figure 4 | North-south profiles of east-west velocity. North-south profiles of the east-west component of the velocity field from the model with unlocked faults (solid lines) reveal that slip is partitioned amongst the different branches and that internal deformation occurs. Velocities from the locked-fault model (dashed lines) widely agree with interseismic GPS velocities[5] (circles with 2σ uncertainties). Inset: Map showing the locations of profiles and GPS sites[5] used for comparison.

Anatolian plate and the Eurasian plate has to be distinguished from the slip rate on the MMF. Slip partitioning on several faults and internal deformation contribute to relative plate motion at the expense of slip on the MMF. Consideration of these mechanisms along with the submarine structural complexities explains the geodetic observations and the geologically derived fault slip rates. The slip rate is variable along the MMF, which indicates strain release during several earthquakes rather than the occurrence of one large event rupturing the whole seismic gap at once. However, the seismic threat to the city of Istanbul being located at a distance of only ~ 20 km from the fault is still serious.

Received 29 June 2009; accepted 1 December 2009; published online 17 January 2010

References

1. Scholz, C. H. The Mechanics of Earthquakes and Faulting 2nd edn (Cambridge Univ. Press, 2002).
2. Le Pichon, X. L., Chamot-Rooke, A., Rangin, C. & Şengör, A. M. C. The North Anatolian fault in the Sea of Marmara. *J. Geophys. Res.* **108**, 2179 (2003).
3. Flerit, F., Armijo, R., King, G. & Meyer, B. The mechanical interaction between the propagating North Anatolian Fault and the back-arc extension in the Aegean. *Earth Planet. Sci. Lett.* **224**, 347–362 (2004).
4. Meade, B. J. et al. Estimates of seismic potential in the Marmara Sea region from block models of secular deformation constrained by GPS measurements. *Bull. Seism. Soc. Am.* **92**, 208–215 (2002).
5. Reilinger, R. et al. GPS constraints on continental deformation in the Africa–Arabia–Eurasia continental collision zone and implications for the dynamics of plate interaction. *J. Geophys. Res.* **111**, B05411 (2006).
6. Laigle, M. et al. A first deep seismic survey in the Sea of Marmara: Deep basins and whole crust architecture and evolution. *Earth Planet. Sci. Lett.* **270**, 168–179 (2008).
7. Armijo, R., Meyer, B., Navarro, S., King, G. & Barka, A. Asymmetric slip partitioning in the Sea of Marmara pull-apart: A clue to propagation processes of the North Anatolian Fault? *Terra Nova* **13**, 80–86 (2002).
8. Armijo, R., Meyer, B., Hubert, A. & Barka, A. Westward propagation of the North Anatolian fault into the northern Aegean: Timing and kinematics. *Geology* **27**, 267–270 (1999).
9. Rockwell, T. K. et al. *International Workshop in Comparative Studies of the North Anatolian Fault and the San Andreas Fault* 11–12 (2006).
10. Rockwell, T. et al. in *Paleoseismology: Historical and Prehistorical Records of Earthquake Ground Effects for Seismic Hazard Assessment*. Vol. 316 (eds Reicherter, K., Michetti, A. M. & Silva, P. G.) 31–54 (Spec. Publs. Geol. Soc., 2009).
11. Youngs, R. R. & Coppersmith, K. J. Implications of fault slip rates and earthquake recurrence models to probabilistic seismic hazard estimates. *Bull. Seism. Soc. Am.* **75**, 939–964 (2003).
12. Erdik, M., Demircioglu, M., Sesetyan, K., Durukal, E. & Siyahi, B. Earthquake hazard in Marmara Region, Turkey. *Soil Dyn. Earthq. Eng.* **24**, 605–631 (2004).
13. Heidbach, O. & Drewes, H. in *New Insights in Structural Interpretation and Modelling* (ed. Nieuwland, D.) 259–272 (Spec. Publs. Geol. Soc., 2003).
14. Bécel, A. et al. Moho, crustal architecture and deep deformation under the North Marmara Trough, from the Seismarmara Leg1 offshore-onshore reflection-refraction survey. *Tectonophysics* **467**, 1–21 (2009).
15. Carton, H. et al. Seismic imaging of the three-dimensional architecture of the Çınarcık Basin along the North Anatolian Fault. *J. Geophys. Res.* **112**, B06101 (2007).
16. Parke, J. R. et al. Interaction between faulting and sedimentation in the Sea of Marmara, western Turkey. *J. Geophys. Res.* **107**, B11 (2002).
17. Seeber, L. et al. Uplift and subsidence from oblique slip: The Ganos-Marmara bend of the North Anatolian Transform, Western Turkey. *Tectonophysics* **391**, 239–258 (2004).
18. Seeber, L. et al. Rapid subsidence and sedimentation from oblique slip near a bend on the North Anatolian transform fault in the Marmara Sea, Turkey. *Geology* **34**, 933–936 (2006).
19. Yaltırak, C. Late Pleistocene uplift history along the southwestern Marmara Sea determined from raised coastal deposits and global sea-level variations. *Mar. Geol.* **190**, 283–305 (2002).
20. Yaltırak, C. & Alpar, B. Evolution of the middle strand of North Anatolian Fault and shallow seismic investigation of the southeastern Marmara Sea (Gemlik Bay). *Mar. Geol.* **190**, 307–327 (2002).
21. McClusky, S. et al. Global positioning system constraints on plate kinematics and dynamics in the eastern Mediterranean and Caucasus. *J. Geophys. Res.* **105**, 5695–5719 (2000).
22. Ambraseys, N. The seismic activity of the Marmara sea region over the last 2000 years. *Bull. Seismol. Soc. Am.* **92**, 1–18 (2002).

Acknowledgements

We thank A. Bécel, M. Laigle and A. Hirn for providing data for the basement topography and Moho, and A. Hirn, K. Fuchs, F. Wenzel and M. Laigle for suggestions. This work was supported by the CEDIM Project at the University of Karlsruhe and GFZ German Research Centre for Geosciences, by the Heidelberg Academy of Sciences and Humanities and by the Task Force VII 'Temporal and Spatial Changes of Stress and Strain' of the International Lithosphere Program.

Author contributions

The modelling and analysis was carried out by T.H., in consultation with O.H. Both authors wrote the manuscript.

Additional information

The authors declare no competing financial interests. Supplementary information accompanies this paper on www.nature.com/naturegeoscience. Reprints and permissions information is available online at http://npg.nature.com/reprintsandpermissions. Correspondence and requests for materials should be addressed to T.H. or O.H.